

Spin glass model of in-context learning

Yuhao Li¹, Ruoran Bai¹, and Haiping Huang^{1,2*}

¹*PMI Lab, School of Physics, Sun Yat-sen University,
Guangzhou 510275, People's Republic of China and*

²*Guangdong Provincial Key Laboratory of Magnetoelectric Physics and Devices,
Sun Yat-sen University, Guangzhou 510275, People's Republic of China*

(Dated: August 6, 2024)

Large language models show a surprising in-context learning ability—being able to use a prompt to form a prediction for a query, yet without additional training, in stark contrast to old-fashioned supervised learning. Providing a mechanistic interpretation and linking the empirical phenomenon to physics are thus challenging and remain unsolved. We study a simple yet expressive transformer with linear attention, and map this structure to a spin glass model with real-valued spins, where the couplings and fields explain the intrinsic disorder in data. The spin glass model explains how the weight parameters interact with each other during pre-training, and most importantly why an unseen function can be predicted by providing only a prompt yet without training. Our theory reveals that for single instance learning, increasing the task diversity leads to the emergence of the in-context learning, by allowing the Boltzmann distribution to converge to a unique correct solution of weight parameters. Therefore the pre-trained transformer displays a prediction power in a novel prompt setting. The proposed spin glass model thus establishes a foundation to understand the empirical success of large language models.

INTRODUCTION

Thanks to earlier breakthroughs in processing natural languages (e.g., translation), vector representation and attention concepts were introduced into machine learning [1–4], which further inspired a recent breakthrough of implementing the self-attention as a feedforward model of information flow, namely transformer [5]. The self-attention captures dependencies between different parts of the input (e.g., image or text), coupled with a simple cost of next-token prediction [6, 7], leading to a revolution in the field of natural language processing [8], so-called large language model (LLM).

One of the astonishing abilities in the transformer is the in-context learning [9], i.e., the pre-trained transformer is able to accomplish previously-unseen complicated tasks by showing a short prompt in the form of instructions and a handful of demonstrations, especially without a need for updating the model parameters. LLMs thus develop a wide range of abilities and skills (e.g., question answering, code generation) [10], which are not explicitly contained in the training dataset and not specially designed to optimize. This remarkable property is achieved only by training for forecasting next tokens and only if corpus and model sizes are scaled up to a huge number [11, 12]. The above characteristics of transformer and the in-context learning (ICL) are in stark contrast to perceptron models in the standard supervised learning context, presenting a formidable challenge for a mechanistic interpretation [13, 14].

To achieve a scientific theory of ICL, previous works focused on optimization via gradient descent dynamics [15, 16], representation capacity [17], Bayesian inference [18, 19], and in particular the pre-training task diversity [19–22]. The theoretical efforts were commonly

based on a single-layer linear attention [15, 21, 23, 24], which revealed that a sufficient pre-training task diversity guarantees the emergence of ICL, i.e., the model can generalize beyond the scope of pre-training tasks.

However, rare connections are established to physics models, which makes a physics model of ICL lacking so far, preventing us from a deep understanding about how ICL emerges from pre-trained model parameters. Here, we treat the transformer learning as a statistical inference problem, and then rephrase the inference problem as a spin glass model, where the transformer parameters are turned into real-valued spins, and the input sequences act as a quenched disorder, which makes the spins strongly interact with each other to lower down the ICL error. There exists a unique spin solution to the model, guaranteeing that the transformer can predict the unknown function embedded in test prompts.

TRANSFORMER WITH LINEAR ATTENTION

We consider a simple transformer structure—a single-layer self-attention transforming an input sequence to an output one. Given an input sequence $\mathbf{X} \in \mathbb{R}^{D \times N}$, where D is the embedding dimension and N is the context length, the self-attention matrix is a softmax function $\text{Softmax}(\mathbf{Q}^T \mathbf{K} / \sqrt{D})$, where $\mathbf{Q} = \mathbf{W}_Q \mathbf{X}$, $\mathbf{K} = \mathbf{W}_K \mathbf{X}$. \mathbf{W}_Q and \mathbf{W}_K are the query and key matrices ($\in \mathbb{R}^{D \times D}$), respectively. \sqrt{D} inside the softmax function makes its argument order of unity. The self-attention refers to the attention matrix generated from the input sequence itself, and allows each element (query) to attend to all other elements in one input sequence, being learnable through pre-training. The softmax function is thus calculated independently for each row. Taking an addi-

tional transformation $\mathbf{Y} = \mathbf{W}_V \mathbf{X}$, where $\mathbf{W}_V \in \mathbb{R}^{D \times D}$ is the value matrix, one can generate the output $\mathbf{Y} = \mathbf{V} \cdot \text{Softmax}(\mathbf{Q}^\top \mathbf{K} / \sqrt{D})$. Hence, this simple transformer implements a function $\varphi_{\text{TF}}(\mathbf{X}) : \mathbb{R}^{D \times N} \rightarrow \mathbb{R}^{D \times N}$.

For simplicity, we further consider a linear attention replacing the computationally expensive softmax, which is still expressive [25]. Defining $\mathbf{W} \equiv \mathbf{W}_Q^\top \mathbf{W}_K$, and choosing $\mathbf{W}_V = \mathbf{1}_D$ ($\mathbf{1}_D$ indicates a $D \times D$ identity matrix), we re-express the linear transformer as $\mathbf{Y} = \frac{1}{D\sqrt{N}} \mathbf{X} \mathbf{X}^\top \mathbf{W} \mathbf{X}$, where \mathbf{X} contains prompts and the query (to be predicted by the transformer), and $\mathbf{W} \in \mathbb{R}^{D \times D}$ is the equivalent weight matrix to be trained, and $\frac{1}{D\sqrt{N}}$ is a normalization coefficient.

We next design the training task as a high-dimensional linear regression, and each example consists of the data $\mathbf{x} \sim \mathcal{N}(0, \mathbf{1}_D)$ and the corresponding label $y = \mathbf{w}^\top \mathbf{x}$, where the latent task weight $\mathbf{w} \sim \mathcal{N}(0, \mathbf{1}_D)$. For the μ -th input matrix, we use N samples as prompts using the same \mathbf{w}^μ yet different \mathbf{x} within the input sequence. An additional sample $\tilde{\mathbf{x}}^\mu$ is regarded as the query whose true label \tilde{y} is masked yet to be predicted by the transformer. The structure of each input matrix \mathbf{X}^μ is thus represented as

$$\mathbf{X}^\mu = \begin{bmatrix} \mathbf{x}_1^\mu & \mathbf{x}_2^\mu & \cdots & \mathbf{x}_n^\mu & \tilde{\mathbf{x}}^\mu \\ y_1^\mu & y_2^\mu & \cdots & y_n^\mu & 0 \end{bmatrix} \in \mathbb{R}^{(D+1) \times (N+1)}. \quad (1)$$

The last element of \mathbf{Y} corresponds to the predicted label to the query $\tilde{\mathbf{x}}^\mu$, i.e., $\hat{y}^\mu = \mathbf{Y}_{D+1, N+1}^\mu$. The goal of ICL is to use the prompt to form a prediction for the query, and the true function governing the linear relationship may be unseen during pre-training, because each μ is generated by an independently-drawn \mathbf{w} during both training and test phases. We consider an ensemble of P sequences, and P is thus called the task diversity. This setting is bit different from that in recent works [19, 21].

The pre-training is carried out by minimizing the mean squared error function, and the total training loss is given by

$$\mathcal{L} = \frac{1}{2P} \sum_{\mu} (\tilde{y}^\mu - \hat{y}^\mu)^2 + \frac{\lambda}{2} \|\mathbf{W}\|^2, \quad (2)$$

where λ controls the weight-decay strength. The generalization error on unseen tasks is written as $\epsilon_g = \mathbb{E}_{\tilde{\mathbf{x}}, \mathbf{x}, \mathbf{w}} (\tilde{y} - \hat{y})^2$, where the ensemble average over all disorders is considered.

SPIN-GLASS MODEL MAPPING

Equation (2) can be treated as a Hamiltonian in statistical physics. The linear attention structure makes the spin-model mapping possible. This proceeds as follows. The prediction to the μ -th input matrix can be recast as $\hat{y}^\mu = (D\sqrt{N})^{-1} \sum_{m,n} \mathbf{C}_{D+1,m}^\mu \mathbf{W}_{m,n} \mathbf{X}_{n,N+1}^\mu$,

where $\mathbf{C}^\mu \equiv \mathbf{X}^\mu \mathbf{X}^{\mu \top}$. Then we define an index mapping $\Gamma : (m, n) \rightarrow i$ to flatten a matrix into a vector. Therefore, one can write $\sigma_i = \Gamma \mathbf{W}_{m,n}$, and $s_i^\mu = (D\sqrt{N})^{-1} \Gamma \mathbf{C}_{D+1,m}^\mu \mathbf{X}_{n,N+1}^\mu$, where $i = (D+1)(m-1)+n$, and finally the prediction as $\hat{y}^\mu = \sum_i s_i^\mu \sigma_i$. Consequently, the loss for each input matrix reads

$$\ell^\mu = \frac{1}{2} \sum_{i,j} s_i^\mu s_j^\mu \sigma_i \sigma_j - \tilde{y}^\mu \sum_i s_i^\mu \sigma_i + \frac{\lambda}{2} \sum_i \sigma_i^2, \quad (3)$$

where we omit the constant term $(\tilde{y}^\mu)^2/2$.

Upon defining $J_{ij}^\mu \equiv -s_i^\mu s_j^\mu$, $h_i^\mu \equiv \tilde{y}^\mu s_i^\mu$, and $\lambda_i^\mu \equiv \lambda - J_{ii}^\mu$, we obtain a spin glass model! The disorder in the pre-training dataset including the diversity in the latent task vectors \mathbf{w} is now encoded into the interactions between spins, and random fields the spins feel. In fact, this is a densely-connected spin glass model, while the coupling and field statistics do not have an analytic expression [26], as they bear a fat tail (Fig. 1). This reminds us of two-body spherical spin model studied in spin glass theory [27, 28], but the current glass model of ICL seems much more complex than the spherical model. The Hamiltonian averaged over all input matrices thus reads

$$\mathcal{H}(\boldsymbol{\sigma}) = - \sum_{i < j} J_{ij} \sigma_i \sigma_j - \sum_i h_i \sigma_i + \frac{1}{2} \sum_i \lambda_i \sigma_i^2, \quad (4)$$

where the effective interaction $J_{ij} \equiv (1/P) \sum_{\mu} J_{ij}^\mu$, the external field $h_i \equiv (1/P) \sum_{\mu} h_i^\mu$ and the regularization factor $\lambda_i \equiv (1/P) \sum_{\mu} \lambda_i^\mu$. By construction, this model reflects the nature of associative memory [29], yet the spin variable is now the underlying parameter of the transformer. To conclude, we derive a spin glass model of ICL, opening a physically appealing route towards the mechanistic interpretation of ICL and even more complex layered transformer.

STATISTICAL MECHANICS ANALYSIS

Because the statistics of couplings and fields has no analytic form, one can use the cavity method, an alternative method to replica trick widely used in spin glass theory. The cavity method is also known as the belief propagation algorithm, working by iteratively solving a closed equation of cavity quantity, e.g., a spin is virtually removed [29]. The cavity method can thus be used on single instances of ICL. The probability of each weight configuration is given by the Gibbs-Boltzmann distribution $P(\boldsymbol{\sigma}) = e^{-\beta \mathcal{H}(\boldsymbol{\sigma})} / Z$, where Z is the partition function, and β is an inverse temperature tuning the energy level. Different weight components are likely strongly-correlated, but the cavity marginal $\eta_{i \rightarrow j}(\sigma_i)$ becomes conditionally independent, which facilitates our derivation of the following self-consistent iteration (namely

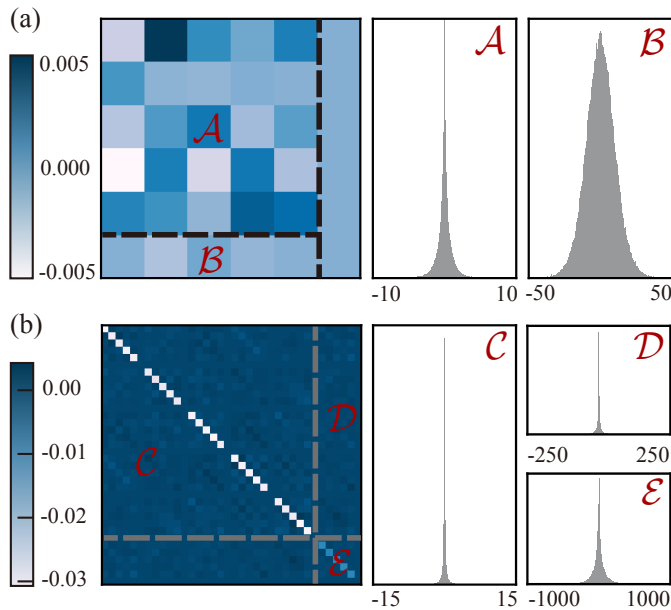


FIG. 1: Statistical properties of the interaction matrix. (a) The \mathbf{S} matrix corresponding to the vector \mathbf{s} has three blocks with different properties: block \mathcal{A} for $m < D + 1, n \neq D + 1$, block \mathcal{B} for $m = D + 1, n \neq D + 1$ and an all-zero vector for $m = D + 1$ (the rightmost column). The statistics is shown in the right panel. (b) The distributions of the elements in different blocks of the symmetric \mathbf{J} matrix. The element in each block J_{ij} is described below. \mathcal{C} : $i \in \mathcal{A}, j \in \mathcal{A}$, and \mathcal{D} : $i \in \mathcal{A}, j \in \mathcal{B}$, and \mathcal{E} : $i \in \mathcal{B}, j \in \mathcal{B}$.

mean-field equation [29]):

$$\eta_{i \rightarrow j}(\sigma_i) = \frac{1}{z_{i \rightarrow j}} e^{\beta h_i \sigma_i - \frac{1}{2} \beta \lambda_i \sigma_i^2} \times \prod_{k \neq i, j} \left[\int d\sigma_k \eta_{k \rightarrow i}(\sigma_k) e^{\beta J_{ik} \sigma_i \sigma_k} \right], \quad (5)$$

where $z_{i \rightarrow j}$ is a normalization constant, and $\eta_{i \rightarrow j}$ is defined as the cavity probability of spin σ_i in the absence of the interaction between spins i and j . After the iteration reaches a fixed point, the marginal probability $\eta_i(\sigma_i)$ of each spin can be calculated by

$$\eta_i(\sigma_i) = \frac{1}{z_i} e^{\beta h_i \sigma_i - \frac{1}{2} \beta \lambda_i \sigma_i^2} \prod_{j \neq i} \int d\sigma_j \eta_{j \rightarrow i}(\sigma_j) e^{\beta J_{ij} \sigma_i \sigma_j}. \quad (6)$$

Because of the continuous nature of spin and weak but dense interactions among spins, we can further simplify the mean-field equation [Eq. (5)], and derive the approximate message passing (AMP) by assuming $\eta_i(\sigma_i) \sim \mathcal{N}(m_i, v_i)$, where (m_i, v_i) is the fixed point of the follow-

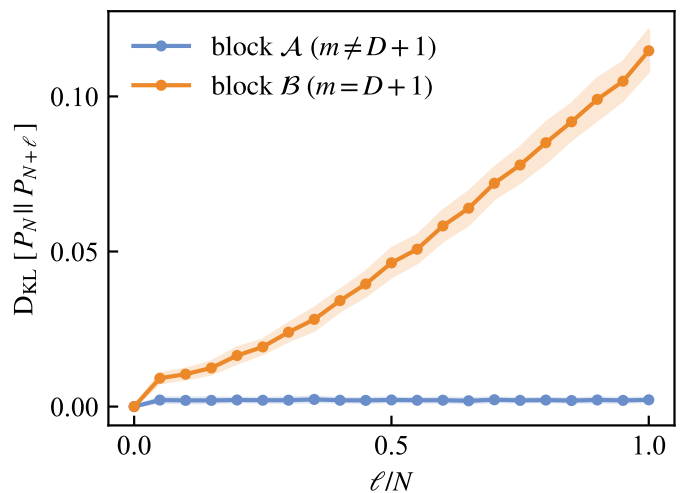


FIG. 2: The KL divergence $D_{\text{KL}}[P_N \| P_{N+\ell}]$ between the original distribution of the elements in blocks \mathcal{A} and \mathcal{B} (see Fig. 1) and that with the prompt length N prolonged by ℓ .

ing iterative equation:

$$m_i = \frac{\beta h_i + \beta \sum_{j \neq i} J_{ij} m_j}{\beta \lambda_i - \beta^2 \sum_{j \neq i} J_{ij}^2 v_j}, \quad (7a)$$

$$v_i = \frac{1}{\beta \lambda_i - \beta^2 \sum_{j \neq i} J_{ij}^2 v_j}. \quad (7b)$$

Technical details of deriving the AMP are given in the supplemental material.

RESULTS

The iteration of the cavity method depends on the specific form of J_{ij} and h_i , that is, on s_i . We first focus on the original form $S_{m,n}$, which is not yet flattened by the Γ map, defined as $S_{m,n} = (D\sqrt{N})^{-1} \mathbf{C}_{D+1,m} \mathbf{X}_{n,N+1}$. The index μ is omitted by meaning an average over all input matrices $\{\mathbf{X}^\mu\}$. The matrix \mathbf{S} is divided into three blocks: the last column is an all-zero vector, while the other two blocks are labeled as \mathcal{A} ($m < D + 1, n \neq D + 1$) and \mathcal{B} ($m = D + 1, n \neq D + 1$) respectively in Fig. 1(a). The statistics of h_i is almost the same as that of s_i [Fig. 1 (a)], since $h_i = \tilde{y} s_i$. However, the key matrix, \mathbf{J} , generated by the outer product of the flattened \mathbf{S} with itself, has three main blocks, labeled as \mathcal{C} , \mathcal{D} , and \mathcal{E} respectively in Fig. 1 (b).

In contrast to traditional spin glass models [27], $P(\mathbf{J})$ does not have an analytic form [26]. For example, the elements in the block \mathcal{C} corresponds to the product of two random variables $z_i z_j$ ($i \neq j$), where each of them is a sum of the product of a few i.i.d. standard normal random variables. Therefore, we provide the numerical estimation of the coupling distribution, which all bear a fat tail [Fig. 1 (b)]. We thus define a new type of

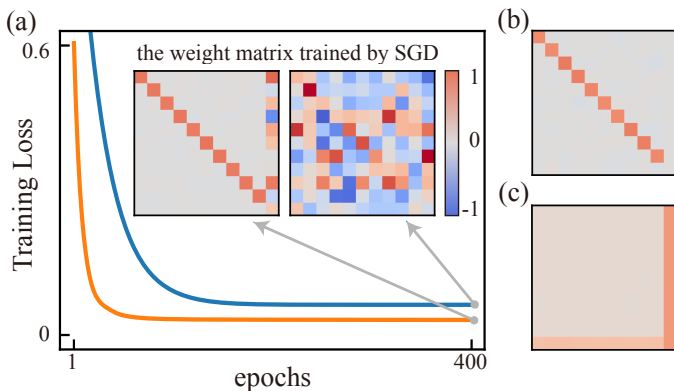


FIG. 3: The optimal weight matrix of ICL. (a) The training loss and the weight matrix \mathbf{W} in the linear attention trained by the stochastic gradient descent (SGD) method. The blue line corresponds to the task diversity $P = 10$, which shows that the model is not well-trained. The orange line corresponds to the case of $P = 1000$, for which the weight matrix is well-trained into a correct diagonal matrix. (b) The weight matrix retrieved from the solution $\{m_i\}$ of AMP. (c) The variance matrix retrieved from the solution $\{v_i\}$ of AMP. The color bars in (b) and (c) are the same with (a).

spin glass model corresponding to ICL, or a metaphor of transformer in large language models. A surprising observation is that the distributions of block \mathcal{A} before and after increasing the prompt length are almost the same, while the block \mathcal{B} seems sensitive to the change of the prompt length [Fig. 2]. As D grows, the part \mathcal{A} will dominate the behavior of the linear attention, which captures the essence of ICL explained below.

To see whether our spin glass model captures the correct structure of the weight matrix in the simple transformer, we first divide the weight matrix \mathbf{W} into blocks in the same way as we do for the input matrix, i.e.,

$$\mathbf{W} = \begin{bmatrix} \mathbf{W}_{11} & \mathbf{W}_{12} \\ \mathbf{W}_{21} & \mathbf{W}_{22} \end{bmatrix} \quad (8)$$

where $\mathbf{W}_{11} \in \mathbb{R}^{D \times D}$, $\mathbf{W}_{12} \in \mathbb{R}^{D \times 1}$, $\mathbf{W}_{21} \in \mathbb{R}^{1 \times D}$, and $\mathbf{W}_{22} \in \mathbb{R}$. In our linear regression task, the prediction of the model to the test query $\tilde{\mathbf{x}}$ can be written as

$$\hat{y} = \mathbf{w}^\top (\mathbf{W}_{11} + \mathbf{w}\mathbf{W}_{21}) \tilde{\mathbf{x}}. \quad (9)$$

To derive the above prediction, we have used 2×2 block matrix form of \mathbf{X} and the fact of i.i.d. $\{\mathbf{x}_\ell\}$. Hence, the weight matrix of a well-trained model must satisfy

$$\mathbf{W}_{11} + \mathbf{w}\mathbf{W}_{21} = \mathbf{1}_D. \quad (10)$$

It is clear that, in the case of $P > 1$, the weights have a unique optimal solution $\mathbf{W}_{11} = \mathbf{1}_D$ and $\mathbf{W}_{21} = 0$.

In the standard stochastic gradient descent (SGD) training process minimizing Eq. (2), a large value of P is needed to make the weight matrix converge to the unique solution, as the training error cannot be precisely reduced

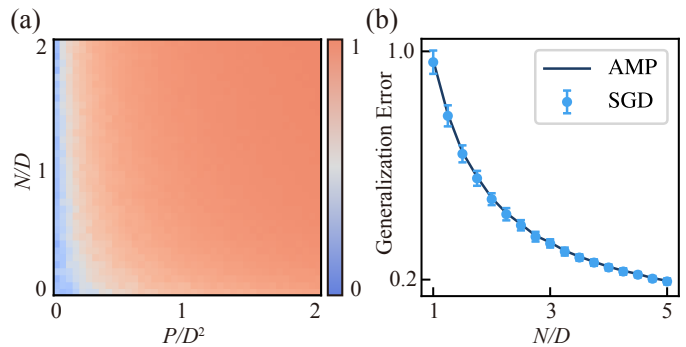


FIG. 4: Results obtained from running the AMP algorithm. (a) The heat map of the contrast \mathcal{C} with $D = 40$, $\lambda = 10$, and $\beta = 100$. (b) The generalization error decreases with the context (prompt) length N , with $D = 40$, $\lambda = 0.1$, $P = 1000$ and $\beta = 100$. All the results of AMP and SGD are averaged over 100 trials.

to zero. In Fig. 3, we show the training loss curves and the weight matrix after the training when the amount of training data $P = 10$ and $P = 1000$ respectively. By iterating the AMP equations [Eq. (7a) and Eq.(7b)], we get a fixed point of $\{m_i\}$ and $\{v_i\}$, transformed back into the matrix form by inverting Γ . We find that the \mathbf{m} matrix exhibits the same property as the weight matrix that is well trained by the SGD. Since the last column of \mathbf{W} is initialized as $\mathcal{N}(0, 1)$ and does not participate in the training, the solution of AMP retains the structure of $m = 0$ and $v = 1$. This result shows that our spin glass model captures the properties of practical SGD training.

To get the phase diagram for single instance pre-training of the transformer, we first define a contrast ratio $\mathcal{C} = (\langle m_{ii}^2 \rangle - \langle m_{ij}^2 \rangle) / \langle m_{ii}^2 \rangle$, $i \neq j$ to measure whether the model is well trained according to the transformed \mathbf{m} matrix. $\mathcal{C} = 1$ means that the model converges to the unique solution, while $\mathcal{C} = 0$ indicates that the model does not learn the features at all. We show a heat map of the contrast with the rescaled number of the data P/D^2 and the rescaled prompt length N/D in Fig. 4 (a). The heat map suggests that when the task diversity increases, a smooth transition to perfect generalization occurs, while keeping a large value of task diversity, increasing the prompt length further lowers down the generalization error, which is consistent with recent empirical works [19] and theoretical works [21] based on random matrix theory (despite a slight different setting). In addition, the AMP result coincides perfectly with the SGD [Fig. 4 (b)], which verifies once again that our spin-glass model of ICL is able to predict an unseen embedded function in the test prompts, which is determined by the ground states of $\mathcal{H}(\boldsymbol{\sigma})$.

CONCLUSION

A fundamental question in large language models is what contributes to the emergence ability of ICL, i.e., why simple next-token prediction based pre-training leads to in-context learning of previously unseen tasks, especially without further tuning the model parameters. Here, we turn the ICL into a spin glass model, and verify the equivalence between the standard SGD training and our statistical mechanic inference. We observe the fat tail distribution of coupling that determines how the model parameters of the transformer interact with each other. The transformer parameters are akin to an ensemble of real-valued spins in physics whose ground state suggests that the model can infer an unknown function from the shown test prompts after a pre-training of input sequences of sufficient task diversity. The phase diagram for single instance learning is also derived by our method, suggesting a continuous ICL transition.

The spin-glass model mapping of a simple transformer with linear attention working on linear regression tasks thus establishes a toy model of understanding emergent abilities of large language models. This work could be potentially generalized to other attention setting, e.g.,

the softmax one. Future exciting directions include explaining the chain-of-thought prompting [12], i.e., decomposition of a complex task into intermediate steps, and more challenging case of hallucination [30], i.e., the model could not distinguish the generated outputs from factual knowledge, or it could not understand what they generate [14]. We speculate that this hallucination may be intimately related to the solution space of the spin glass model given a fixed complexity of training dataset, e.g., spurious states in a standard associative memory model, as implied by Eq. (4). These open questions are expected to be addressed in the near future, thereby enhancing robustness and trustworthiness of AI systems.

ACKNOWLEDGMENTS

This research was supported by the National Natural Science Foundation of China for Grant number 12122515, and Guangdong Provincial Key Laboratory of Magnetolectric Physics and Devices (No. 2022B1212010008), and Guangdong Basic and Applied Basic Research Foundation (Grant No. 2023B1515040023).

Derivation of Relaxed Belief Propagation and Approximate Message Passing

In this appendix, we derive the approximate message passing equation in the main text. To proceed, we first define $\xi_{i \rightarrow j} = \sum_{k \neq i, j} \beta J_{ik} \sigma_k$, and $G(\xi_{i \rightarrow j}) = e^{\sigma_i \xi_{i \rightarrow j}}$. The cavity equation [Eq. (5)] can be written as

$$\begin{aligned}
 \eta_{i \rightarrow j}(\sigma_i) &= \frac{1}{z_{i \rightarrow j}} e^{\beta h_i \sigma_i - \frac{1}{2} \beta \lambda_i \sigma_i^2} \int \prod_{k \neq i, j} [d\sigma_k \eta_{k \rightarrow i}(\sigma_k)] G(\xi_{i \rightarrow j}) \\
 &= \frac{1}{z_{i \rightarrow j}} e^{\beta h_i \sigma_i - \frac{1}{2} \beta \lambda_i \sigma_i^2} \int d\hat{\xi}_{i \rightarrow j} \hat{G}(\hat{\xi}_{i \rightarrow j}) \prod_{k \neq i, j} \int d\sigma_k \eta_{k \rightarrow i}(\sigma_k) \exp \left[i \hat{\xi}_{i \rightarrow j} (\beta J_{ik} \sigma_k) \right] \\
 &\approx \frac{1}{z_{i \rightarrow j}} e^{\beta h_i \sigma_i - \frac{1}{2} \beta \lambda_i \sigma_i^2} \int d\hat{\xi}_{i \rightarrow j} \hat{G}(\hat{\xi}_{i \rightarrow j}) \prod_{k \neq i, j} \exp \left[i \hat{\xi}_{i \rightarrow j} \beta J_{ik} m_{k \rightarrow i} - \frac{1}{2} \hat{\xi}_{i \rightarrow j}^2 \beta^2 J_{ik}^2 v_{k \rightarrow i} \right].
 \end{aligned} \tag{11}$$

In the second line of Eq. (11), we insert the Fourier transform of $G(\xi)$, $\hat{G}(\hat{\xi}_{i \rightarrow j})$ denotes the corresponding inverse transform, and in the third line, we use the Taylor expansion of exponential function, which requires us to define the following mean $m_{i \rightarrow j}$ and variance $v_{i \rightarrow j}$ of the message (the cavity marginal probability):

$$m_{i \rightarrow j} = \int d\sigma_i \eta_{i \rightarrow j}(\sigma_i) \sigma_i, \quad v_{i \rightarrow j} = \int d\sigma_i \eta_{i \rightarrow j}(\sigma_i) \sigma_i^2 - m_{i \rightarrow j}^2. \tag{12}$$

Then, we reformulate $G(\xi)$ by its inverse Fourier transform $\hat{G}(\hat{\xi}_{i \rightarrow j})$, and obtain

$$\begin{aligned}
\eta_{i \rightarrow j}(\sigma_i) &= \frac{1}{z_{i \rightarrow j}} e^{\beta h_i \sigma_i - \frac{1}{2} \beta \lambda_i \sigma_i^2} \int d\xi_{i \rightarrow j} G(\xi_{i \rightarrow j}) \int d\hat{\xi}_{i \rightarrow j} \\
&\times \exp \left[-\frac{1}{2} \left(\beta^2 \sum_{k \neq i, j} J_{ik}^2 v_{k \rightarrow i} \right) \hat{\xi}_{i \rightarrow j}^2 + i \left(\beta \sum_{k \neq i, j} J_{ik} m_{k \rightarrow i} - \xi_{i \rightarrow j} \right) \hat{\xi}_{i \rightarrow j} \right] \\
&= \frac{1}{z_{i \rightarrow j}} e^{\beta h_i \sigma_i - \frac{1}{2} \beta \lambda_i \sigma_i^2} \int d\xi_{i \rightarrow j} \exp \left[-\frac{1}{2} \frac{1}{V_{i \rightarrow j}} \xi_{i \rightarrow j}^2 + \left(\frac{M_{i \rightarrow j}}{V_{i \rightarrow j}} + \sigma_i \right) \xi_{i \rightarrow j} - \frac{M_{i \rightarrow j}^2}{2V_{i \rightarrow j}} \right] \\
&= \frac{1}{z_{i \rightarrow j}} \exp \left[-\frac{1}{2} (\beta \lambda_i - V_{i \rightarrow j}) \sigma_i^2 + (\beta h_i + M_{i \rightarrow j}) \sigma_i \right],
\end{aligned} \tag{13}$$

where we have defined

$$M_{i \rightarrow j} = \beta \sum_{k \neq i, j} J_{ik} m_{k \rightarrow i}, \quad V_{i \rightarrow j} = \beta^2 \sum_{k \neq i, j} J_{ik}^2 v_{k \rightarrow i}. \tag{14}$$

Combining Eq. (13) and Eq. (12), one can immediately calculate the mean

$$m_{i \rightarrow j} = \frac{\int d\sigma_i \sigma_i \exp \left[-\frac{1}{2} (\beta \lambda_i - V_{i \rightarrow j}) \sigma_i^2 + (\beta h_i + M_{i \rightarrow j}) \sigma_i \right]}{\int d\sigma_i \exp \left[-\frac{1}{2} (\beta \lambda_i - V_{i \rightarrow j}) \sigma_i^2 + (\beta h_i + M_{i \rightarrow j}) \sigma_i \right]} = \frac{\beta h_i + M_{i \rightarrow j}}{\beta \lambda_i - V_{i \rightarrow j}}, \tag{15}$$

and the variance

$$v_{i \rightarrow j} = \frac{\int d\sigma_i \sigma_i^2 \exp \left[-\frac{1}{2} (\beta \lambda_i - V_{i \rightarrow j}) \sigma_i^2 + (\beta h_i + M_{i \rightarrow j}) \sigma_i \right]}{\int d\sigma_i \exp \left[-\frac{1}{2} (\beta \lambda_i - V_{i \rightarrow j}) \sigma_i^2 + (\beta h_i + M_{i \rightarrow j}) \sigma_i \right]} - m_{i \rightarrow j}^2 = \frac{1}{\beta \lambda_i - V_{i \rightarrow j}}. \tag{16}$$

Finally, we arrive at the iterative equation called relaxed belief propagation:

$$\begin{cases} M_{i \rightarrow j} = \beta \sum_{k \neq i, j} J_{ik} m_{k \rightarrow i}, \\ V_{i \rightarrow j} = \beta^2 \sum_{k \neq i, j} J_{ik}^2 v_{k \rightarrow i}, \end{cases} \quad \begin{cases} m_{i \rightarrow j} = \frac{\beta h_i + M_{i \rightarrow j}}{\beta \lambda_i - V_{i \rightarrow j}}, \\ v_{i \rightarrow j} = \frac{1}{\beta \lambda_i - V_{i \rightarrow j}}. \end{cases} \tag{17}$$

After the relaxed belief propagation equation converges, we get further the marginal probability as

$$\begin{aligned}
\eta_i(\sigma_i) &= \frac{1}{z_i} e^{\beta h_i \sigma_i - \frac{1}{2} \beta \lambda_i \sigma_i^2} \prod_{j \neq i} \left\{ \int d\sigma_j \exp \left[-\frac{1}{2} (\beta \lambda_j - V_{j \rightarrow i}) \sigma_j^2 + (\beta h_j + \beta J_{ij} \sigma_i + M_{j \rightarrow i}) \sigma_j \right] \right\} \\
&= \frac{1}{z_i} e^{\beta h_i \sigma_i - \frac{1}{2} \beta \lambda_i \sigma_i^2} \prod_{j \neq i} \exp \left[\frac{(\beta h_j + \beta J_{ij} \sigma_i + M_{j \rightarrow i})^2}{2(\beta \lambda_j - V_{j \rightarrow i})} \right] \\
&= \frac{1}{z_i} \exp \left[-\frac{1}{2} \left(\beta \lambda_i - \sum_{j \neq i} \beta^2 J_{ij}^2 v_{j \rightarrow i} \right) \sigma_i^2 + \left(\beta h_i + \sum_{j \neq i} \beta J_{ij} m_{j \rightarrow i} \right) \sigma_i \right].
\end{aligned} \tag{18}$$

Therefore, $\eta_i(\sigma_i)$ can be computed as a Gaussian distribution $\mathcal{N}(m_i, v_i)$, where

$$m_i = \frac{\beta h_i + \beta \sum_{j \neq i} J_{ij} m_{j \rightarrow i}}{\beta \lambda_i - \beta^2 \sum_{j \neq i} J_{ij}^2 v_{j \rightarrow i}}, \quad v_i = \frac{1}{\beta \lambda_i - \beta^2 \sum_{j \neq i} J_{ij}^2 v_{j \rightarrow i}}. \tag{19}$$

By using the following identities $M_i = M_{i \rightarrow j} + \beta J_{ij} m_{j \rightarrow i}$ and $V_i = V_{i \rightarrow j} + \beta^2 J_{ij}^2 v_{j \rightarrow i}$, we further find that

$$m_i - m_{i \rightarrow j} = \frac{\beta J_{ij} m_{j \rightarrow i} (\beta \lambda_i - V_i) + \beta^2 J_{ij}^2 v_{j \rightarrow i} (\beta h_i + M_i)}{\beta^2 \lambda_i^2 - 2\beta \lambda_i V_i + V_i^2} \sim \mathcal{O} \left(\frac{1}{D^2} \right), \tag{20}$$

and

$$v_i - v_{i \rightarrow j} = \frac{\beta^2 J_{ij}^2 v_{j \rightarrow i}}{\beta^2 \lambda_i^2 - 2\beta \lambda_i V_i + V_i^2} \sim \mathcal{O} \left(\frac{1}{D^4} \right). \tag{21}$$

As a consequence, we can further reduce the relaxed belief propagation equation to the AMP equation

$$m_i = \frac{\beta h_i + \beta \sum_{j \neq i} J_{ij} m_j}{\beta \lambda_i - \beta^2 \sum_{j \neq i} J_{ij}^2 v_j}, \quad v_i = \frac{1}{\beta \lambda_i - \beta^2 \sum_{j \neq i} J_{ij}^2 v_j}. \quad (22)$$

This AMP equation saves N -fold space complexity for running the algorithm if we record N as the number of spins in the system. The AMP equation was first discovered in a statistical mechanics analysis of signal transmission problem [31], and is also rooted in the Thouless–Anderson–Palmer equation in glass physics [29, 32].

* Electronic address: huanghp7@mail.sysu.edu.cn

- [1] Yoshua Bengio, Réjean Ducharme, Pascal Vincent, and Christian Janvin. A neural probabilistic language model. *J. Mach. Learn. Res.*, 3:1137–1155, 2003.
- [2] Tomas Mikolov, Ilya Sutskever, Kai Chen, Greg Corrado, and Jeffrey Dean. Distributed representations of words and phrases and their compositionality. In *Proceedings of the 26th International Conference on Neural Information Processing Systems - Volume 2*, NIPS’13, pages 3111–3119, Red Hook, NY, USA, 2013. Curran Associates Inc.
- [3] Kyunghyun Cho, Bart van Merriënboer, Caglar Gulcehre, Dzmitry Bahdanau, Fethi Bougares, Holger Schwenk, and Yoshua Bengio. Learning phrase representations using rnn encoder-decoder for statistical machine translation. In *Proceedings of the 2014 Conference on Empirical Methods in Natural Language Processing (EMNLP)*, pages 1724–1734. Association for Computational Linguistics, 2014.
- [4] Dzmitry Bahdanau, Kyunghyun Cho, and Yoshua Bengio. Neural machine translation by jointly learning to align and translate. In *ICLR 2015 : International Conference on Learning Representations 2015*, 2015.
- [5] Ashish Vaswani, Noam Shazeer, Niki Parmar, Jakob Uszkoreit, Llion Jones, Aidan N. Gomez, Łukasz Kaiser, and Illia Polosukhin. Attention is all you need. In *Proceedings of the 31st International Conference on Neural Information Processing Systems*, NIPS’17, pages 6000–6010, Red Hook, NY, USA, 2017. Curran Associates Inc.
- [6] Eran Malach. Auto-regressive next-token predictors are universal learners. *arXiv:2309.06979*, 2023.
- [7] Chan Li, Junbin Qiu, and Haiping Huang. Meta predictive learning model of languages in neural circuits. *Phys. Rev. E*, 109:044309, 2024.
- [8] Sébastien Bubeck, Varun Chandrasekaran, Ronen Eldan, John A. Gehrke, Eric Horvitz, Ece Kamar, Peter Lee, Yin Tat Lee, Yuan-Fang Li, Scott M. Lundberg, Harsha Nori, Hamid Palangi, Marco Tulio Ribeiro, and Yi Zhang. Sparks of artificial general intelligence: Early experiments with gpt-4. *arXiv:2303.12712*, 2023.
- [9] Tom Brown, Benjamin Mann, Nick Ryder, Melanie Subbiah, Jared D Kaplan, Prafulla Dhariwal, Arvind Neelakantan, Pranav Shyam, Girish Sastry, Amanda Askell, Sandhini Agarwal, Ariel Herbert-Voss, Gretchen Krueger, Tom Henighan, Rewon Child, Aditya Ramesh, Daniel Ziegler, Jeffrey Wu, Clemens Winter, Chris Hesse, Mark Chen, Eric Sigler, Mateusz Litwin, Scott Gray, Benjamin Chess, Jack Clark, Christopher Berner, Sam McCandlish, Alec Radford, Ilya Sutskever, and Dario Amodei. Language models are few-shot learners. In H. Larochelle, M. Ranzato, R. Hadsell, M.F. Balcan, and H. Lin, editors, *Advances in Neural Information Processing Systems*, volume 33, pages 1877–1901. Curran Associates, Inc., 2020.
- [10] Alec Radford, Jeff Wu, Rewon Child, David Luan, Dario Amodei, and Ilya Sutskever. Language models are unsupervised multitask learners. *OpenAI blog*, 1:9, 2019.
- [11] Jared Kaplan, Sam McCandlish, Tom Henighan, Tom B Brown, Benjamin Chess, Rewon Child, Scott Gray, Alec Radford, Jeffrey Wu, and Dario Amodei. Scaling laws for neural language models. *arXiv:2001.08361*, 2020.
- [12] Jason Wei, Yi Tay, Rishi Bommasani, Colin Raffel, Barret Zoph, Sebastian Borgeaud, Dani Yogatama, Maarten Bosma, Denny Zhou, Donald Metzler, Ed H. Chi, Tatsunori Hashimoto, Oriol Vinyals, Percy Liang, Jeff Dean, and William Fedus. Emergent abilities of large language models. *Transactions on Machine Learning Research*, 2022.
- [13] Micah Goldblum, Anima Anandkumar, Richard Baraniuk, Tom Goldstein, Kyunghyun Cho, Zachary C Lipton, Melanie Mitchell, Preetum Nakkiran, Max Welling, and Andrew Gordon Wilson. Perspectives on the state and future of deep learning - 2023. *arXiv:2312.09323*, 2023.
- [14] Haiping Huang. Eight challenges in developing theory of intelligence. *Front. Comput. Neurosci.*, 18:1388166, 2024.
- [15] Johannes Von Oswald, Eyvind Niklasson, Ettore Randazzo, João Sacramento, Alexander Mordvintsev, Andrey Zhmoginov, and Max Vladymyrov. Transformers learn in-context by gradient descent. In *International Conference on Machine Learning*, pages 35151–35174, 2023.
- [16] Alberto Bietti, Vivien Cabannes, Diane Bouchacourt, Herve Jegou, and Leon Bottou. Birth of a transformer: A memory viewpoint. *arXiv:2306.00802*, 2023.
- [17] Shivam Garg, Dimitris Tsipras, Percy S Liang, and Gregory Valiant. What can transformers learn in-context? a case study of simple function classes. *Advances in Neural Information Processing Systems*, 35:30583–30598, 2022.
- [18] Sang Michael Xie, Aditi Raghunathan, Percy Liang, and Tengyu Ma. An explanation of in-context learning as implicit bayesian inference. *arXiv:2111.02080*, 2021.
- [19] Allan Raventós, Mansheej Paul, Feng Chen, and Surya Ganguli. Pretraining task diversity and the emergence of non-bayesian in-context learning for regression. *Advances in Neural Information Processing Systems*, 36, 2024.
- [20] Yingcong Li, Muhammed Emrullah Ildiz, Dimitris Papailiopoulos, and Samet Oymak. Transformers as algorithms: Generalization and stability in in-context learning. In *International Conference on Machine Learning*, pages 19565–19594,

2023.

- [21] Yue M. Lu, Mary I. Letey, Jacob A. Zavatone-Veth, Anindita Maiti, and Cengiz Pehlevan. Asymptotic theory of in-context learning by linear attention. *arXiv:2405.11751*, 2024.
- [22] Jingfeng Wu, Difan Zou, Zixiang Chen, Vladimir Braverman, Quanquan Gu, and Peter L. Bartlett. How many pretraining tasks are needed for in-context learning of linear regression? *arXiv:2310.08391*, 2024. in ICLR 2024.
- [23] Ekin Akyürek, Dale Schuurmans, Jacob Andreas, Tengyu Ma, and Denny Zhou. What learning algorithm is in-context learning? investigations with linear models. *arXiv:2211.15661*, 2022.
- [24] Ruiqi Zhang, Spencer Frei, and Peter L. Bartlett. Trained transformers learn linear models in-context. *Journal of Machine Learning Research*, 25(49):1–55, 2024.
- [25] Kwangjun Ahn, Xiang Cheng, Minhak Song, Chulhee Yun, Ali Jadbabaie, and Suvrit Sra. Linear attention is (maybe) all you need (to understand transformer optimization). *arXiv:2310.01082*, in ICLR, 2024.
- [26] M. D. Springer and W. E. Thompson. The distribution of products of beta, gamma and gaussian random variables. *SIAM Journal on Applied Mathematics*, 18(4):721–737, 1970.
- [27] A. Crisanti and H. J. Sommers. The spherical p-spin interaction spin glass model: the statics. *Zeitschrift für Physik B Condensed Matter*, 87(3):341–354, 1992.
- [28] Giacomo Gradenigo, Maria Chiara Angelini, Luca Leuzzi, and Federico Ricci-Tersenghi. Solving the spherical p-spin model with the cavity method: equivalence with the replica results. *Journal of Statistical Mechanics: Theory and Experiment*, 2020(11):113302, 2020.
- [29] Haiping Huang. *Statistical Mechanics of Neural Networks*. Springer, Singapore, 2022.
- [30] Sebastian Farquhar, Jannik Kossen, Lorenz Kuhn, and Yarin Gal. Detecting hallucinations in large language models using semantic entropy. *Nature*, 630(8017):625–630, 2024.
- [31] Yoshiyuki Kabashima. A cdma multiuser detection algorithm on the basis of belief propagation. *Journal of Physics A: Mathematical and General*, 36(43):11111, 2003.
- [32] P. W. Anderson D. J. Thouless and R. G. Palmer. Solution of 'solvable model of a spin glass'. *Phil. Mag.*, 35(3):593–601, 1977.